ISSN 0208-7774 TRIBOLOGIA 5/2020 p. 27–38
DOI: 10.5604/01.3001.0014.6956

Anna M. RYNIEWICZ[*], Konrad MAZUR[**], Łukasz BOJKO[***], Wojciech RYNIEWICZ[****]

INFLUENCE OF THE POSITION OF THE MANDIBLE ON STRESSES AND DISPLACEMENTS WITHIN THE STRUCTURES OF THE TEMPOROMANDIBULAR JOINT

WPŁYW POŁOŻENIA ŻUCHWY NA NAPRĘŻENIA I PRZEMIESZCZENIA W STRUKTURACH STAWU SKRONIOWO-ŻUCHWOWEGO

Key words: temporomandibular joint, modeling, strength simulations.

Abstract: A model of the temporomandibular joint (TMJ) was developed using the finite element method (FEM). The aim of the procedure is to identify reduced stresses and resultant displacements in the TMJ and to evaluate the transfer of contact loads for the three articulation states of the mandible that represent the activity of the joint. The study mapped the layered structure of the bio-bearing with different strength parameters of the tissues and synovial fluid. The model was loaded with the forces generated by the mandibular abduction muscles during chewing. Our method allowed for the assessment of the transfer of physiological loads within the temporomandibular joint. It enabled the functional analysis of the articular disc and articular surfaces when lubricating with the synovial fluid and showed compressive stimulation of bone structures. Under load transfer conditions, the maximum values of reduced stresses are located not in the immediate friction zone, but in the structures of the compact and spongy bone.

Słowa kluczowe: staw skroniowo-żuchwowy, modelowanie, symulacje wytrzymałościowe.

Streszczenie: Opracowano model stawu skroniowo-żuchwowego (SSŻ) z wykorzystaniem metody elementów skończonych (MES). Celem jest identyfikacja naprężeń zredukowanych i przemieszczeń wypadkowych w SSŻ oraz ocena przeniesienia obciążeń kontaktowych dla trzech stanów artykulacyjnych żuchwy, które są reprezentatywne dla czynności tego stawu. W badaniu odwzorowano warstwową budowę biołożyska o zróżnicowanych parametrach wytrzymałościowych tkanek oraz cieczy synowialnej. Model obciążono siłami generowanymi przez mięśnie odwodzące żuchwę w warunkach żucia pokarmów. Zaproponowana metoda pozwoliła na ocenę przeniesienia obciążeń fizjologicznych w stawie skroniowo-żuchwowym. Umożliwiła analizę funkcjonalną krążka stawowego i powierzchni stawowych w warunkach smarowania cieczą synowialną oraz wskazała na stymulację kompresyjną struktur kostnych. W warunkach przenoszenia obciążeń maksymalne wartości naprężeń zredukowanych zlokalizowane są nie w bezpośredniej strefie tarcia, ale w strukturach kości korowej i gąbczastej.

[*] ORCID: 0000-0003-2469-6527. Jagiellonian University Medical College, Faculty of Medicine, Dental Institute, Department of Dental Prosthodontics, Montelupich 4 Street, 31-155 Cracow, Poland.

[**] AGH University of Science and Technology, Faculty of Mechanical Engineering and Robotics, Mickiewicza 30 Ave., 30-059 Cracow, Poland.

[***] ORCID: 0000-0002-6024-458X. AGH University of Science and Technology, Faculty of Mechanical Engineering and Robotics, Mickiewicza 30 Ave., 30-059 Cracow, Poland.

[****] ORCID: 0000-0002-9140-198X. Jagiellonian University Medical College, Faculty of Medicine, Dental Institute, Department of Dental Prosthodontics, Montelupich 4 Street, 31-155 Cracow, Poland.

INTRODUCTION

Temporomandibular dysfunctions are a common disorder of the stomatognathic system. The factors responsible for the development of the disease are as follows: excessive muscle tension caused by stress, prolonged and excessive load on the tissues of the system, hormonal and metabolic factors, unconscious tightening and grinding of the teeth, and lowered occlusion **[L. 1]**. About 50-80% of people suffer from temporomandibular dysfunction **[L. 2, 3]**. Masticatory organ disorders are the subject of medical and clinical research that also includes biomechanics of the stomatognathic system **[L. 4–7]**.

Diagnostics and treatment of the stomatognathic system require knowledge about the biomechanics of the temporomandibular joint and its functions within the masticatory organ. The temporomandibular joint (TMJ) is the only paired joint **[L. 8–10]**. The heads of the mandible are coupled with the mandibular stem and its branches. The joint is made up of an articular fossa within the temporal bone, an articular tubercle of the zygomatic process of the temporal bone constituting the acetabulum and an articular head located on the condylar process of the mandible. There is an articular disc between these structures (**Fig. 1**). The disc is made of the fibrous cartilage. Its thickness is not the same as it is a reflection of the articular surfaces. The disc divides the joint into two separate spaces that interact functionally. The joint is surrounded by the joint capsule. The joint capsule is strengthened with fibres that make up the joint ligaments. On the entire circumference, the disc is connected with the articular capsule and the condylar process of the mandibular head by the medial and lateral collateral ligaments. The main dynamic complex includes the mandible with the muscular complex and the temporomandibular joints, and the movements are controlled by stimuli sent from the nerve endings in the periodontium, muscles, and joints, as well as from the mucosa of the mouth and tongue. There are three types of movements in the temporomandibular joint. During mouth opening and closing – referred to as the hinge movement – the mandibular heads rotate around a movable transverse axis. The axis moves forward when opening and backward when closing the mouth. The mandibular head not only rotates like a hinge, but also glides along the articular disc, and therefore has no fixed rotation point. The mandible can slide back and forth in a gliding motion. The articular disc and mandibular head can also slide back and forth without even opening the mouth.

The grinding movement consists in the rotation of the mandible around the vertical axis. The mandibular head slides forward, while the opposite head rotates around the vertical axis that runs through it. These movements are characteristic of human temporomandibular joints and are a perfect adaptation to the performed functions. Biomechanics of the joints allows for the articulation of speech, facial expressions, as well as food intake and chewing. Chewing is the most important function of the stomatognathic system that causes the greatest stress. Numerous literature reports determine occlusive forces within the range of 200–3500 N **[L. 9, 12]**. Occlusal forces released between the teeth in adults are the greatest in the posterior segment which is closest to the axis of the mandibular hinge movement and decrease from the molars to the incisors. The structure of the temporomandibular joint varies individually, i.e. it also depends on age and the condition of the teeth **[L. 5, 13–19]**.

The aim of the study is to identify reduced stresses and resultant displacements in the TMJ and to evaluate the transfer of contact loads for three articulation states of the mandible, with the maximum activity of the masticatory muscles.

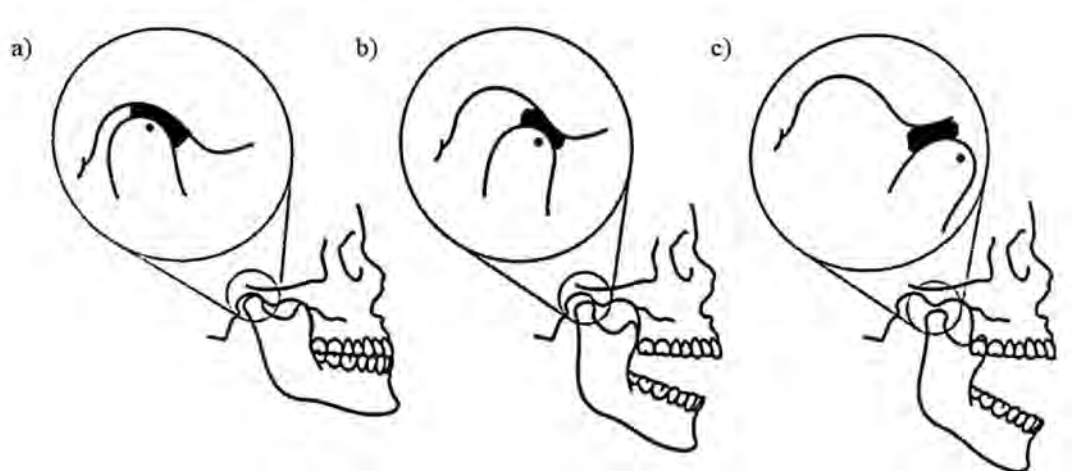

Fig. 1. The position of the articular disc depending on the articulation of the mandible: a) during occlusion, b) in partial abduction, c) in maximum abduction [L. 11]

Rys. 1. Pozycje krążka stawowego w zależności od stanu artykulacyjnego żuchwy: a) w zwarciu, b) w częściowym odwiedzeniu, c) w maksymalnym odwiedzeniu **[L. 11]**

MATERIAL AND METHOD

The material for the analysis is a model of the normal TMJ created on the basis of clinical 3D mapping of the bony articular structures developed by the Organization for Research, Information and Systems of the Faculty of Engineering, the University of Tokyo **[L. 20]**. On the basis of the MR image, the model was supplemented with cartilaginous-fibrous structures from which the articular surfaces and the disc are built. Spatial modelling was carried out using Autodesk Inventor Professional 2017, and numerical modelling using Ansys Workbench 19.2 (**Fig. 2**) **[L. 21]**. The introduction of cartilaginous fibrous structures into the model required the adoption of non-displacement contact between the bony structures of the head and the cartilage structures that build the articular surfaces of the head, as well as between the acetabular bone structures and the fibrous cartilage structures of the articular fossa and articular tubercle. The articular disc was permanently medially and laterally fixed to the poles of the condylar process. In this way, the function of the collateral ligament (disc ligament), which medially and laterally connects the disc with the mandibular head, was mapped. It allows slight hinge movements of the mandibular head relative to the disc and keeps the disc on the mandibular head. A slip was modelled due to the presence of synovial fluid in the articular cavities. A sliding contact between the articulating surfaces of the joint was adopted, in the presence of fluid, with the friction coefficient of $\mu = 0.01$ **[L. 22, 23]**. The model was simplified by omitting the articular capsule and the adoption of an isotropic tissue structure. Assuming elastic deformations, mechanical properties were assigned to the model structures (**Tab. 1**). The model was divided into tetrahedral finite elements. The network of elements was compacted in the areas of contact between the articular surfaces and the disc. The model introduces three articulation states of the mandible that represent the function of the TMJ. The first state of occlusion, i.e. the adduction of the mandible to the maxilla, in which the occlusal surfaces are parallel to each other and the articular disc is located in the articular fossa (**Fig. 2a**). The second state represents the situation when the mandible is partially abducted and the articular disc has moved towards the tubercle (**Fig. 2b**). The third state is the simulation of maximum mandibular abduction – the maximum opening of the mouth. The occlusal surfaces form an angle of 30º and the disc is located on the articular tubercle (**Fig. 2c**). A spatial system of loads and restraints was projected on the model, simulating the conditions of chewing (**Fig. 3**). The mandible was subjected to the loads generated by the muscles, i.e. forces located in the zones of attachments. Values of the forces were determined on the basis of the adopted cross-sections (**Tab. 2**) **[L. 11]**. The following muscles are included: the temporal muscle, the attachment of which is located on the coronoid process of the mandible (marking A), the masseter muscle, the attachment of which is located on the masseter tuberosity of the mandibular branch on the outer surface of the mandibular angle (marking C), the medial pterygoid muscle, which is attached to the pterygoid tuberosity on the inner surface of the

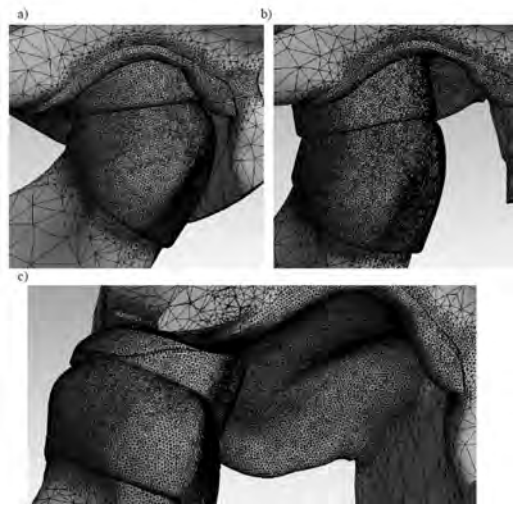

Fig. 2. Numerical model of the temporomandibular joint during: a) mandibular occlusion, b) partial abduction, c) maximum abduction

Rys. 2. Model numeryczny stawu skroniowo-żuchwowego w stanie: a) zwarcia żuchwy, b) w częściowym odwiedzeniu, c) w maksymalnym odwiedzeniu

Table. 1. Mechanical properties of the model structures

Tabela 1. Właściwości mechaniczne struktur modelu

Joint structure	Young's modulus E, MPa		Poisson's ratio ν	
	literature	assumed in calculation	literature	assumed in calculation
Cortical bone	10000–20000	18600	0.29–0.30	0.29
Spongy bone	50–100	60	0.38–0.40	0.38
Hyaline cartilage	1.2–2.7	2.1	0.28–0.38	0.36
Fibrocartilage	1.9–2.8	2.5	0.30–0.38	0.36
Synovial fluid	0.01–0.02	0.01	0.40–0.49	0.47
Tendons and ligaments	10–50	30	0.30–0.35	0.30

mandibular angle (marking D), the lateral pterygoid muscle, whose fibres penetrate into the articular disc and the attachment is located in the pterygoid fovea on the condylar process of the mandible (marking B). Based on literature reports on forces of the masticatory muscles, the angles of deviation for the indicated vector locations were determined during adduction of the mandible **[L. 11]**. Then, the geometric parameters characterizing the position of the muscle attachments were calculated for the three articulatory states of the mandible assessed in the study (**Tab. 3**).

In the model, the occlusal surfaces (marking F) and the upper surface of the temporal bone (marking G) were fixed (**Fig. 3**). The disc was fixed medially and laterally to the poles of the condylar process (H_1 and H_2 markings).

Table 2. Forces of the muscles lifting the mandible for the adopted transverse cross-sections
Tabela 2. Siły mięśni unoszących żuchwę dla założonych przekrojów poprzecznych

Muscle	Marking the location of trailers	Cross section, mm^2	Load, N
temporal	A	560	224
masseter	C	485	194
medial pterygoid	D	325	130
lateral pterygoid	B	335	134

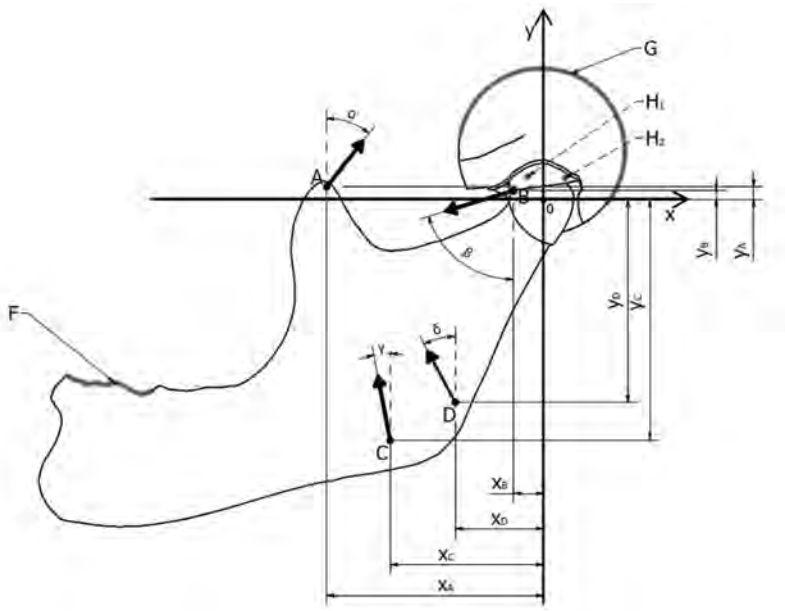

Fig. 3. Loads and restraints of the TMJ model during occlusion
Rys. 3. Obciążenia i utwierdzenia modelu SSŻ w warunkach zwarcia

Table 3. Geometric parameters characterizing the location of muscle attachments in the adopted coordinate system
Tabela 3. Geometryczne parametry charakteryzujące położenie przyczepów mięśni w przyjętym układzie współrzędnych

The position of the mandible	Muscle attachment point	Deviation from the vertical axis y, °	Distance from y axis, mm	Distance from the x axis, mm
Occlusion	A	36	1.3	-38.5
	B	84	2.3	-2.5
	C	10	-45.5	-27.0
	D	25	-38.0	-15
Partial abduction – opening 15°	A	39	-7.0	-37.8
	B	84.2	1.7	-29
	C	14	-50.2	-16.5
	D	28	-40.3	-6.4
Complete abduction – opening 30°	A	42	-15.1	-35.4
	B	84.5	1.0	-3.2
	C	18.5	-52.6	-5.2
	D	32	-40.7	2.4

RESULTS AND DISCUSSION

The results of the calculations are presented in the form of maps presenting distribution of reduced stress in the temporomandibular joint (according to the Huber-Mises-Hencky (HMH) hypothesis) for the mandible in the occlusion (**Fig. 4**), the partially abducted mandible (**Fig. 5**), and the completely opened (**Fig. 6**). The highest values of reduced stresses are located in the bony zone of the mandibular head. For each of the models, stress concentrations in the frontal part of the mandibular head reach similar values. The values of stress concentrations are as follows: for the model presenting occlusion – 15 MPa, for the model with partial abduction – 19.9 MPa, and for the model in the opening state – 22.6 MPa. In the area of the posterior mandibular head, they have the following lower values for the considered positions: the highest values are 3–5 MPa in occlusal conditions, and 2–3 MPa in partial abduction and 3–4 MPa in completely abduction. In the articular disc and layers of cartilage that build the articular surfaces, regardless of the variant of the position of the mandible, the reduced stresses decrease to the value of 1–2.1 MPa. In the central zone, where the disc is compressed, the reduced stress is 1.2 MPa for the model of occlusion, and it increases when the mandible is abducted at an angle of 15° – 1.9 MPa and 2.1 MPa during the maximum abduction of the mandible.

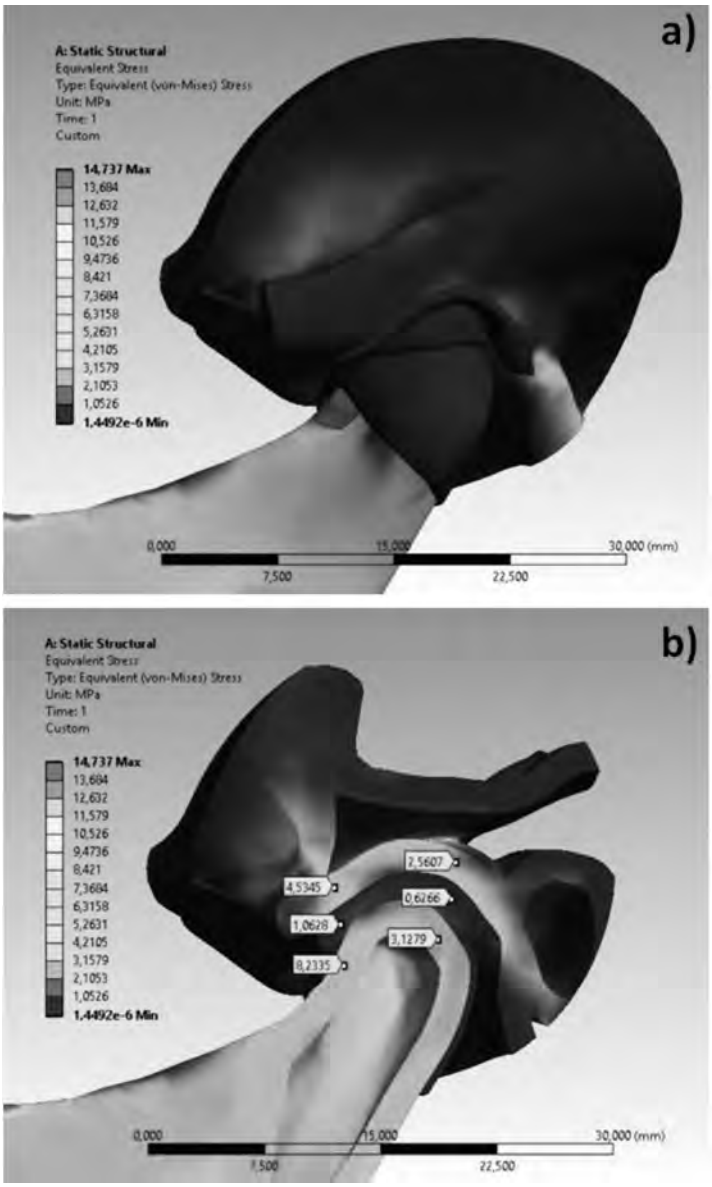

Fig. 4. A map of reduced stresses in the temporomandibular joint during occlusion of the mandible: a) a 3D model view, b) the sagittal cross-section

Rys. 4. Mapa naprężeń zredukowanych w stawie skroniowo-żuchwowym w stanie zwarcia żuchwy: a) widok modelu 3D, b) przekrój w płaszczyźnie strzałkowej

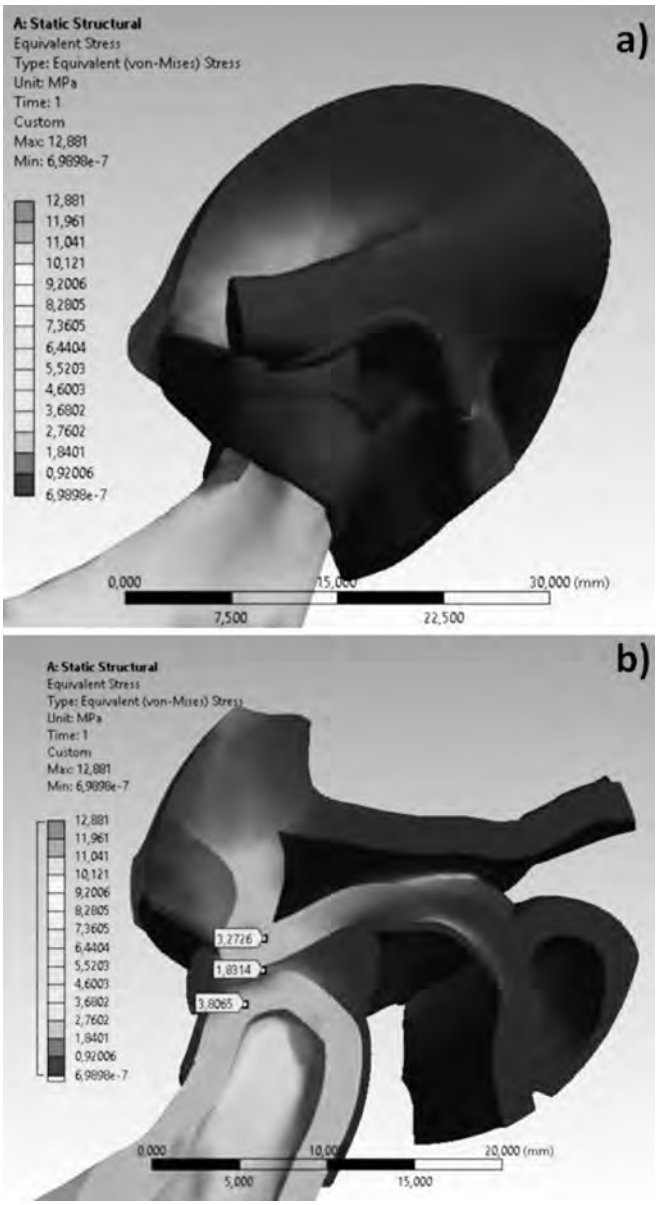

Fig. 5. A map of reduced stresses in the temporomandibular joint during incomplete mouth opening: a) a 3D model view, b) the sagittal cross-section

Rys. 5. Mapa naprężeń zredukowanych w stawie skroniowo-żuchwowym w stanie niecałkowitego rozwarcia żuchwy: a) widok modelu 3D, b) przekrój w płaszczyźnie strzałkowej

Larger values penetrate the bony structure of the articular fossa in the temporal bone and the tubercle on the zygomatic process of the temporal bone and depend on the location of the mandibular head resulting from the variant of its location. For occlusion conditions, the stress concentration in the articular fossa reaches the highest values of 8–9 MPa, with incomplete opening the concentration in the posterior structure of the tubercle, they reach the value of 5–6 MPa, and in conditions of complete abduction of the mandible in the central structure of the tubercle, they reach the value of 3–4 MPa.

In the structures of the temporomandibular joint made of the fibrous cartilage, the values of reduced stresses are much lower compared to the bone structures.

Numerical simulation allowed us to determine the distribution of resultant displacements in the temporomandibular joint for three states of the mandible position (**Fig. 7**). In each model, the greatest resultant displacement occurs in the posterior part of the mandibular head. During occlusion, the values reach 1.31 mm, when the mandible is partially abducted, and the maximum value of displacement is 1.58 mm, and when fully opened, the displacements are 2.75 mm.

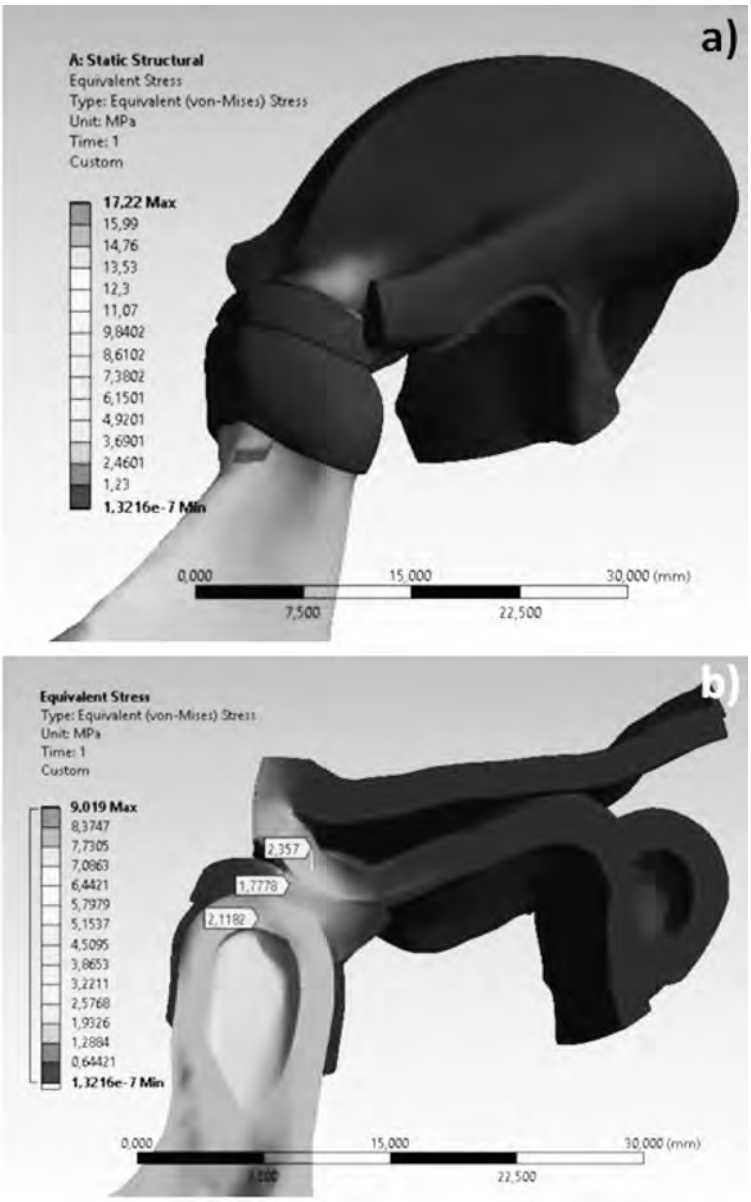

Fig. 6. A map of reduced stresses in the temporomandibular joint – the mandible is completely abducted: a) a 3D model view, b) the sagittal cross-section

Rys. 6. Mapa naprężeń zredukowanych w stawie skroniowo-żuchwowym – żuchwa całkowicie odwiedziona: a) widok modelu 3D, b) przekrój w płaszczyźnie strzałkowej

During occlusion, the disc is compressed (**Fig. 8**). The greatest displacement is reported at the point of contact of the mandibular head with the peripheral structure of disc and amounts to 1.16 mm. Directional displacements on the periphery of the disc in the X and Z axes are positive, and their maximum values remain in the following ranges: in the X axis 0.14–0.17 mm, and in the Z axis 0.64–0.74 mm (**Fig. 8b, d**). Y-axis directional displacements are negative in the range -0.17 to -0.25 mm (**Fig. 8c**). In contact with the cartilage of the articular fossa, displacements decrease to 0.15 mm.

When the mandible is fully abducted, the disc is stretched and compressed in the area of contact with the mandibular head and the articular tubercle (**Fig. 9**). The maximum displacement in this anterior zone of the disc is 2.21 mm. X-axis directional displacements indicate that the disc in the front and rear zones is stretched. These displacements are in the range from -0.14 to -0.04 mm (**Fig. 9b**). There are slight compressive displacements of 0.04 mm in the middle of the disc. Directional displacements in the Y axis indicate tensile stress (**Fig. 9c**). The range of negative displacements is from

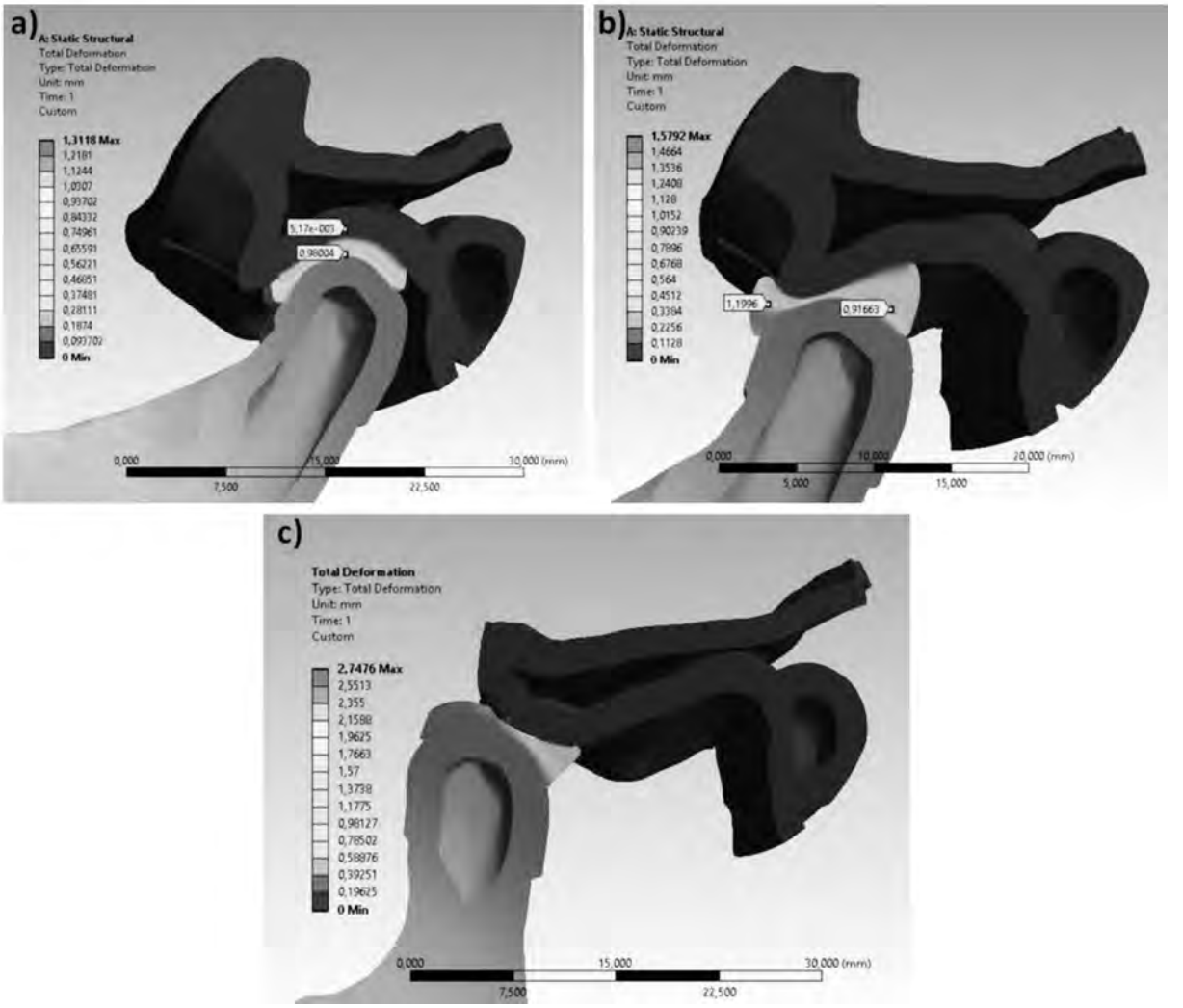

Fig. 7. Maps of accidental displacements in the temporomandibular joint in the sagittal cross-section, in three articulation states: a) in the state of occlusion of the mandible, b) in the state of partial abduction, c) in maximum abduction

Rys. 7. Mapy przemieszczeń wypadkowych w stawie skroniowo-żuchwowym w przekroju sagitalnym, w trzech stanach artykulacji: a) w stanie zwarcia żuchwy, b) w stanie częściowego odwiedzenia, c) w maksymalnym odwiedzeniu

-1.69 to -1.44 mm. Directional displacements in the Z axis indicate compression, while the maximum displacement values occur in the front zone and amount to 1.33 mm (**Fig. 9d**). In the zone of contact with the articular surface of the fossa, the displacements disappear.

In the model with partial abduction of the mandible, the disc in contact with the head is stretched in the anterior part to a maximum value of 1.40 mm, compressed in the middle zone, and tensile displacements of the smallest value of 0.12 mm occur in the posterior zone in contact with the head. The directional displacements in the X axis indicate that the front disc structure is slightly stretched in the range from -0.07 to -0.03 mm, and in the rear disc structure, it is compressed with a maximum value of 0.14 mm (**Fig. 10b**). The directional displacements in the Y axis indicate that the front and rear disc structure is stretched in the range from -1.13 to -0.28 mm (**Fig. 10c**). The directional displacements in the Z axis indicate that the disc is compressed in the range from 0.65 to 0.97 mm (**Fig. 10d**). In this model, in the zone of contact with acetabular cartilage, displacements disappear.

In the cartilaginous articular structure of the acetabulum, the maximum displacement was observed in the articular tubercle, in the case of opening, equal to 0.74 mm. Slightly lower values of 0.64 mm were found under conditions of incomplete opening. Displacements disappear in the bone structures of the temporal bone.

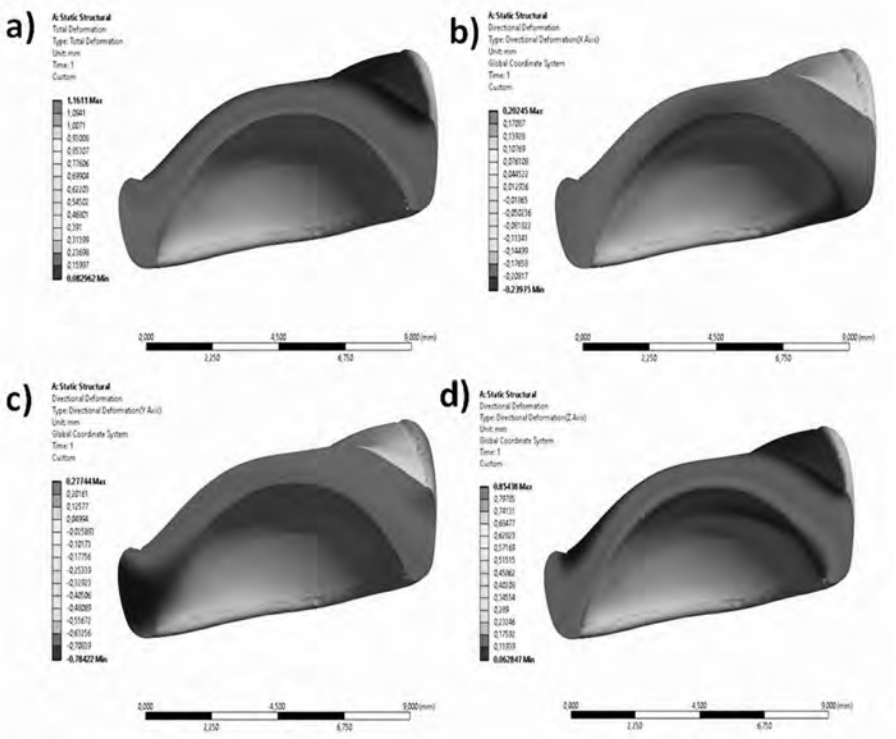

Fig. 8. A map of displacements in the articular disc during occlusion: a) resultant displacements, b) directional displacements in the X axis, c) directional displacements in the Y axis, d) directional displacements in the Z axis

Rys. 8. Mapa przemieszczeń w krążku stawowym podczas zwarcia: a) przemieszczenia wypadkowych, b) przemieszczenia kierunkowe w osi X, c) przemieszczenia kierunkowe w osi Y, d) przemieszczenia kierunkowe w osi Z

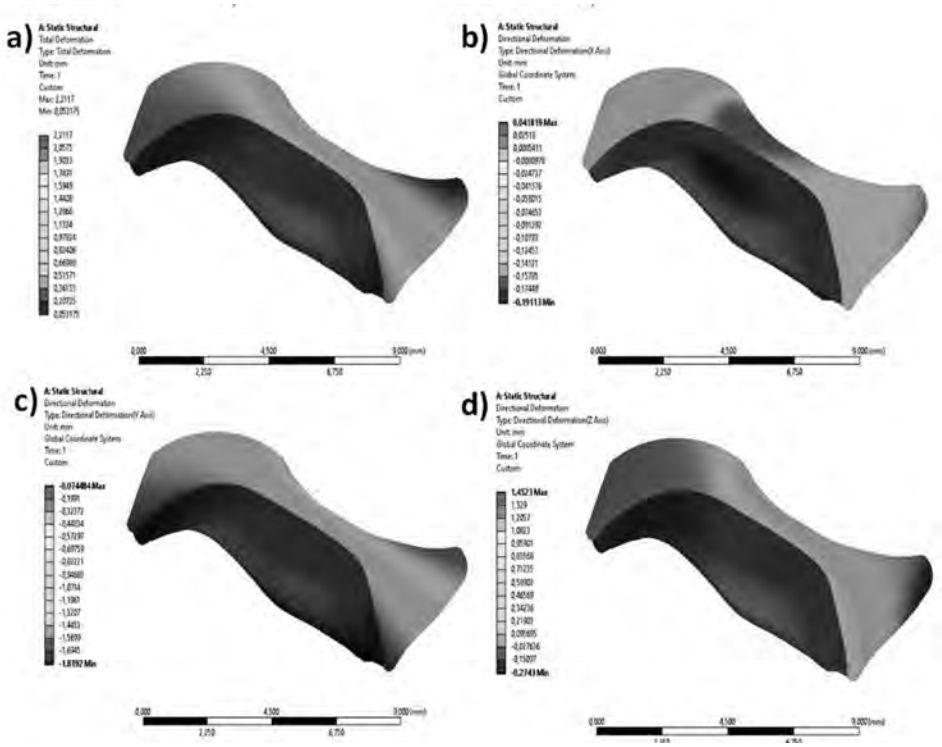

Fig. 9. A map of displacements in the articular disc during complete opening: a) resultant displacements, b) directional displacements in the X axis, c) directional displacements in the Y axis, d) directional displacements in the Z axis

Rys. 9. Mapa przemieszczeń w krążku stawowym podczas całkowitego rozwarcia: a) przemieszczenia wypadkowych, b) przemieszczenia kierunkowe w osi X, c) przemieszczenia kierunkowe w osi Y, d) przemieszczenia kierunkowe w osi Z

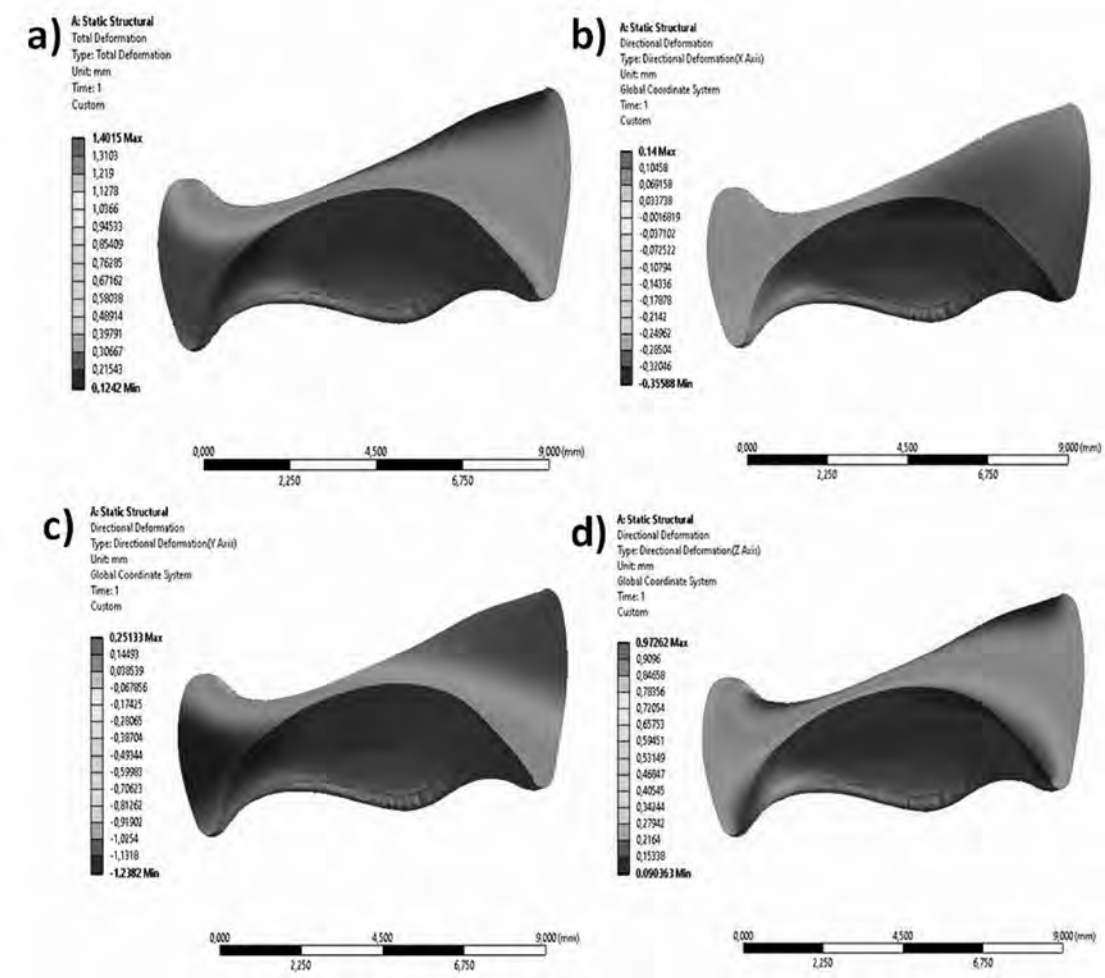

Fig. 10. A map of displacements in the articular disc during partial abduction: a) resultant displacements, b) directional displacements in the X axis, c) directional displacements in the Y axis, d) directional displacements in the Z axis

Rys. 10. Mapa przemieszczeń w krążku stawowym podczas częściowego odwiedzenia: a) przemieszczenia wypadkowych, b) przemieszczenia kierunkowe w osi X, c) przemieszczenia kierunkowe w osi Y, d) przemieszczenia kierunkowe w osi Z

SUMMARY AND CONCLUSIONS

The model study allowed us to determine the reduced HMH stresses and resultant displacements within the temporomandibular joint. Maximum stresses are located in the bone structures. Stress concentrations occur in the anterior bony structure of the mandibular head. The stresses pass through the structures from the fibrous cartilage to the temporal bone. The greatest stresses appear when the mandible is adducted and the smallest when the mouth is fully opened. Stresses in the articular disc reach the greatest values in the zone of the contact of the mandibular head with the articular disc. Comparing the results for the three states of mandible articulation, we can conclude that, in the model in which the mouth is fully open, the greatest displacements and the greatest stresses occur in the structures of the fibrous tissue. The transfer of loads within the joint must be carried out without exceeding the threshold of physiological strength of the fibrous tissue. Functional disorders of the stomatognathic system may be the result of overload **[L. 2, 6, 7, 16]**. In the calculations, the distribution of reduced stresses and resultant displacements did not exceed the permissible values.

The resulting displacements are varied, with the greatest values in the posterior part of the mandibular head.

During occlusion and incomplete abduction of the mandible, the articular disc is compressed mainly in the medial part, and when the mouth is fully open it is compressed and stretched.

Significant displacements were reported in the cartilage articular structures of the temporal bone and the head of the mandible at the point of contact with the disc. The articular disc and articular structures of the temporal bone and the mandibular head absorb contact loads of the stomatognathic system.

The proposed method allowed for the assessment of the transfer of physiological loads within the

temporomandibular joint **[L. 4, 16, 24-26]**. It enabled the functional analysis of the articular disc and articular surfaces when lubricating with synovial fluid and showed the compressive stimulation of bone structures. Under load transfer conditions, the maximum values of reduced stresses are located not in the immediate friction zone, but in the subchondral structures, in the spongy and compact bone.

ACKNOWLEDGEMENT

This work is financed by AGH University of Science and Technology, Faculty of Mechanical Engineering and Robotics: subvention No. 16.16.130.942.

REFERENCES

1. Ferreira F.M., Cézar Simamoto-Júnior P., Soares C.J., Ramos A.M.D.A.M., Fernandes-Neto A.J.: Effect of Occlusal Splints on the Stress Distribution on the Temporomandibular Joint Disc. Brazilian dental journal, 28, 3(2017), pp. 324–329.
2. Roberts W.E., Stocum D.L.: Part II: Temporomandibular joint (TMJ) – Regeneration, degeneration, and adaptation. Current Osteoporosis Reports, 16, 4 (2018), pp. 369–379.
3. Ryniewicz A.M., Ryniewicz A.: Analiza mechanizmu smarowania stawów człowieka w badaniach in vitro oraz in vivo. Przegląd elektrotechniczny, 90, 5(2014), pp. 142–145.
4. Tappert L., Baldit A., Laurent C., Ferrari M., Lipinski P.: Acquisition of accurate temporomandibular joint disc external shape and internal microstructure. In 8th World Congress of Biomechanics, 2018.
5. Segù M., Manfredini D.: Temporomandibular Joint Disorders in the Elderly. In Oral Rehabilitation for Compromised and Elderly Patients. Springer, Cham., 2019, pp. 63–79.
6. Mumme M., Barbero A., Miot S., Wixmerten A., Feliciano S., Wolf F., Asnaghi A.M., Baumhoer D., Bieri O., Kretzschmar M., Pagenstert G., Haug M., Schaefer D.J., Martin I., Jacob M.: Nasal chondrocyte-based engineered autologous cartilage tissue for repair of articular cartilage defects: an observational first-in-human trial. The Lancet, 388, 10055(2016), pp. 1985–1994.
7. Musumeci G., Szychlinska M.A., Mobasheri A.: Age-related degeneration of articular cartilage in the pathogenesis of osteoarthritis: molecular markers of senescent chondrocytes. Histol Histopathol, 30, 1 (2015), pp. 1–12.
8. Lippert H.: Anatomy. Volume 2. Wrocław: Medical Publisher Urban & Partner, 1998.
9. Majewski S.W.: Gnatofizjologia stomatologiczna: normy okluzji i funkcje układu stomatognatycznego. Wydawnictwo Lekarskie PZWL, 2018.
10. McMillan B.: Wielki atlas anatomii człowieka. Grupa Wydawnicza Foksal, 2013.
11. Margielewicz J., Kijak E., Lipski T., Pihut M., Kosiewicz J., Liet-Kijak D.: Badania modelowe równowagi biostatycznej narządu żucia człowieka. Centrum Inżynierii Biomedycznej, Gliwice 2012.
12. Sakaguchi R.L., Powers J.M.: Craig's restorative dental materials. Elsevier Health Sciences, Philadelphia 2012.
13. Ikeda R., Ikeda K.: Directional characteristics of incipient temporomandibular joint disc displacements: A magnetic resonance imaging study. American Journal of Orthodontics and Dentofacial Orthopedics, 149, 1 (2016), pp. 39–45.
14. Moreno-Hay I., Okeson, J.P.: Single event versus recurrent luxation of the temporomandibular joint. The Journal of the American Dental Association, 150, 3 (2019), pp. 225–229.
15. Tu K.H., Chuang H.J., Lai L.A., Hsiao M.Y.: Ultrasound imaging for temporomandibular joint disc anterior displacement. Journal of medical ultrasound, 26, 2 (2018), p. 109.
16. Balenton N., Khakshooy A., Chiappelli F.: Lubricin: Toward a Molecular Mechanism for Temporomandibular Joint Disorders. In Temporomandibular Joint and Airway Disorders. Springer, Cham, 2018, pp. 61–70.
17. Shaik S., Parker M.E.: The assessment of osseous changes in the temporomandibular joint using Cone Beam Computed Tomography. South African Dental Journal, 73, 4 (2018), pp. 259–261.
18. Balatgek T.L., Demerjian G.G., Sims A.B., Patel M.: CBCT and MRI of Temporomandibular Joint Disorders and Related Structures. In Temporomandibular Joint and Airway Disorders, Springer, Cham, 2018, pp. 201–218.
19. Ibi M.: Inflammation and Temporomandibular Joint Derangement. Biological and Pharmaceutical Bulletin, 42, 4 (2019), pp. 538–542.
20. BodyParts3D, © The Database Center for Life Science licensed under CC Attribution-Share Alike 2.1 Japan.
21. Ryniewicz A.M., Ryniewicz A.: Analysis of the Mechanism of Lubrication of the Temporomandibular Joint. Tribologia, 1 (2020), pp. 63–73.

22. Ryniewicz A.M.: Identification, modelling and biotribology of human joints. AGH University of Science and Technology Press, 2011.
23. Sahoo P., Das S.K., Davim J.P.: Tribology of materials for biomedical applications. In Mechanical Behaviour of Biomaterials. Woodhead Publishing, 2019, pp. 1–45.
24. Wei F.: Behavioral, Functional, and Shape Assessment for Temporomandibular Joint, 2018.
25. Liu Z., Qian Y., Zhang Y., Fan Y.: Effects of several temporomandibular disorders on the stress distributions of temporomandibular joint: a finite element analysis. Computer methods in biomechanics and biomedical engineering, 19, 2(2016), pp. 137–143.
26. Shu J.H., Yao J., Zhang Y.L., Chong D.Y., Liu Z.: The influence of bilateral sagittal split ramus osteotomy on the stress distributions in the temporomandibular joints of the patients with facial asymmetry under symmetric occlusions. Medicine, 97, 25(2018), p. 11204.